ARCHIVES OF ELECTRICAL ENGINEERING VOL. 72(4), pp. 1073–1087 (2023)

DOI 10.24425/aee.2023.147427

A dual-stator brushless doubly-fed generator for wind power application

HAO LIU[1], YAKAI SONG[1], CHUNLAN BAI[2], GUOFENG HE[1], XIAOJU YIN[3] ✉

[1] *School of Electrical and Control Engineering, Henan University of Urban Construction Longxiang Avenue, Xincheng District, Pingdingshan, China*

[2] *School of Surveying and Urban Spatial Information, Henan University of Urban Construction Longxiang Avenue, Xincheng District, Pingdingshan, China*

[3] *Department of Renewable Energy, Shenyang Institute of Engineering No. 18 Puchang Road, Shenbei New District, Shenyang, China*

e-mail: liuhao368368@163.com, syk200503@126.com, 86963263@qq.com, hgf@zju.edu.cn, ✉xiaojuyin@outlook.com

(Received: 14.04.2023, revised: 13.09.2023)

Abstract: A novelty dual-stator brushless doubly-fed generator (DSBDFG) with magnetic-barrier rotor structure is put forward for application in wind power. Compared with a doubly-fed induction generator, the DSBDFG has virtues of high reliability and low maintenance costs because of elimination of brush and sliprings components. Therefore, the proposed structure has tremendous potential as a wind power generator to apply in wind power. According to the operating principle of electric machine, the DSBDFG is studied in wind power application. At first, the topology, the winding connecting, the rotor structure, the power flow chart of different operating models and the variable speed capability of electric machine are discussed and analyzed. Then, a 50 kW DSBDFG is designed. Based on the principal dimension of the design electric machine, the electromagnetic characteristics of the DSBDFG with different running modes are analyzed and calculated to adopt the numerical method. From the result, it meets the requests of electromagnetic consistency and winding connecting in the design electric machine. Meanwhile, it confirms the proposed DSBDFG has the strong ability of speed regulation.

Key words: doubly-fed machines, dual-stator, electromagnetic analysis, operational characteristics modes, wind power generation

1. Introduction

In the past few years, wind power generation with the fossil energy growing tension and the environmental issues growing prominent has developed rapidly in [1–3]. Wind energy is a kind of inexhaustible and sustainable renewable clean energy. Therefore, wind power generation has attracted worldwide attention, attracting many scholars and experts at home and abroad to be devoted to its research. China has attached great importance to develop wind power generation. Meanwhile, China has also formulated the "14th Five-Year Plan for Wind Power Development", which requires the goal of carbon neutrality, high efficient utilization, low-carbon and safety in [4]. By the end of the year 2022, China's cumulative installed wind power capacity had met the requirement of 396 GW, making it one of the fastest-developing and most significant country in the world [5]. Based on the wind power progression at present, the wind turbine is provided with the requirements of high power density, small volume and high reliability to apply offshore wind power generation in [6–8].

Brushless doubly-fed machines (BDFMs) have strengths of high reliability, low maintenance costs and improved low-voltage crossing capability because of the elimination of brushes and slip-ring parts [9–13]. Meanwhile, the BDFMs are suitable for slow running because the number of electric machine pole-pairs is about two times greater than traditional doubly-fed induction machines (DFIMs) under the same armature diameter in [14, 15]. Therefore, the BDFMs have attracted a lot of attention in various areas, for instance, the wind power generator in [16], pump in [17], ship in [18], rotary transformer in [19], and electric vehicle [20]. However, the prominent problem of BDFMs is low torque density in [21]. The paper is putting forward a novelty magnetic barrier rotor double stator brushless doubly-fed generator (DSBDFG) to enhance the torque density. The proposed electric machine improves the torque density due to dual-stator structure, which is verified in [22] and [23]. Therefore, the DSBDFG is one of the developing trends in the wind power generation development.

Compared with traditional brushless doubly-fed generators (BDFGs), the DSBDFG has differences in both principle and structure. The flux density distribution of double air-gaps in the DSBDFG is more complicated than the traditional BDFGs because of the existence of double stator and magnetic-barrier rotor structures. Therefore, further in-depth study is needed. The DSBDFG has been researched on electromagnetic design, mechanical design, cooling system and temperature rise, which have achieved some achievements. Reference [24] mainly proposed a modular scheme with the mechanic structure of DSBDFG, and it is verified by the finite element analysis. Reference [25] mainly introduces an analytic method to solve the DSBDFG air-gap flux density. In order to avoid the risk of overheating, a novel equivalent thermal network model is proposed to calculate and analyze the temperature rise of the double-stator BDFG, and the results were verified by the finite element method (FEM) in [26]. However, the control systems of proposed DSBDFG has been less studied. In order to study on its control system in the future, it is necessary to deeply analyze the working principle, power flow and running mode of the DSBDFG. The purpose of this study is to improve the theory of kind of electric machine as soon as possible. Meanwhile, it accelerates the promotion of the DSBDFG to be applied in the wind power generation.

The paper mainly studies the operational characteristics and power flow of the DSBDFG with magnetic-barrier rotor. Based on the structure and working principle of electric machine, the winding connecting and power flow of the DSBDFG are analyzed. Then, the DSBDFG with

magnetic-barrier rotor is designed. According to the principal dimension of the electric machine, the different running modes of the DSBDFG are calculated and discussed to adopt the FEM. From the result analysis and comparison, it meets the design requirements and electromagnetic characteristic consistency of the DSBDFG. Meanwhile, it also confirms the proposed DSBDFG with magnetic-barrier rotor has the strong ability of speed regulation.

2. Topology and principle of DSBDFG

The DSBDFG configuration is depicted in Fig. 1, in which has two different pole-pairs number windings in external/internal stator, namely power and control windings. The power winding (PW) is directly connected to power grid. However, the control winding (CW) joins to the power grid get through bidirectional inverter, as the grid side converter (GSC) and the machine side converter (MSC), as shown in Fig. 2, where p_p and f_p represent the pole pairs number and

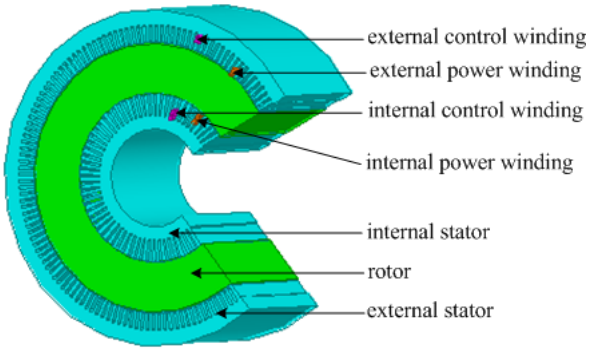

Fig. 1. DSBDFG configuration

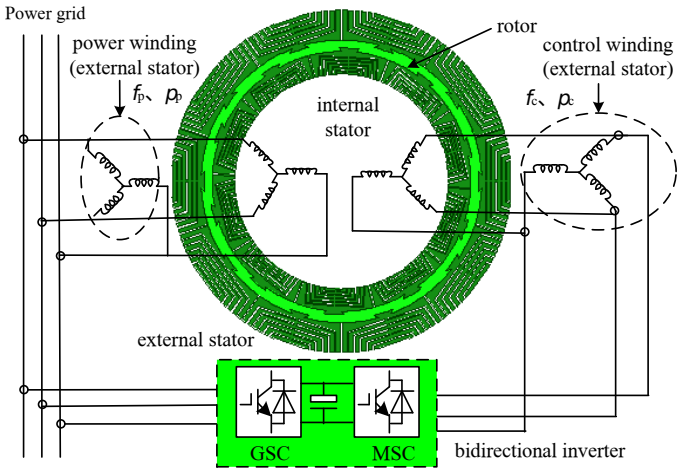

Fig. 2. Winding parallel connection

power source frequency of power windings, p_c and f_c represent the pole pairs number and power source frequency of control windings, respectively. These windings rely on the rotor to carry out the field modulation and coupling. The rotor adopts the back to back structure, which plays the role of modulating and coupling between the stator's power and control windings. The electric machine speed is represented in Eq. (1):

$$n_r = 60 \cdot \frac{f_p \pm f_c}{p_p + p_c}, \tag{1}$$

where: n_r stands for the electric machine speed, "+" stands for the power source phase sequence of power windings is the same with that of control windings, and "-" stands for the power source phase sequence of power windings is the opposite with that of control windings. When p_p, p_c and f_p of the electric machine are confirmed, the electric machine speed is varied with f_c. When f_c is equal to zero, it is called natural synchronous speed. When f_c is less than zero, it is called sub-synchronous speed. Otherwise, it is called super-synchronous speed.

2.1. Stator winding connection

The DSBDFG has two sets of pole-pairs number different windings in internal and external stator, respectively. The internal/external stator windings are partitioned into power and control windings. The power windings of external and internal stators are used to adopt the series/parallel connection. The control windings of internal and external stators also may adopt the parallel/series connection. Therefore, there are four connection modes in the power and control windings of internal and external stators, namely power windings series (PWS) and control windings parallel (CWP), PWS and control windings series (CWS), power windings parallel (PWP) and CWP, and PWP and CWS. The series windings should meet the requirements, including the same wire gauge, the same electromotive force (EMF) phase angle. The requirements of series windings are expressed as follows:

$$\begin{cases} U_N = E_o + E_{\text{in}} \\ d_o = d_{\text{in}} \\ \theta_o = \theta_{\text{in}} \end{cases}, \tag{2}$$

where: E_o expresses the winding EMF of external stator, E_{in} expresses the winding EMF of internal stator, U_N expresses the voltage rating, d_o expresses the winding wire diameter of external stator, d_{in} expresses the internal stator winding wire diameter, θ_o expresses the external stator winding EMF phase angle, and θ_{in} expresses the internal stator winding EMF phase angle.

The parallel windings should meet the requirements of the same EMF amplitude and phase angle. The requirements of parallel windings are expressed as follows:

$$\begin{cases} E_o = E_{\text{in}} \\ \theta_o = \theta_{\text{in}} \end{cases}. \tag{3}$$

The paper is researched on the power and control windings of the internal and external stators in the DSBDFG are all adopted parallel connection, which is indicated in Fig. 2.

2.2. Rotor structure

The rotor configuration is shown in Fig. 3. It consists of internal and external magnetic-barriers of rotor and non-magnetic ring. The external magnetic-barrier of the rotor plays the role of field modulation and coupling between the external stator's power and control windings. The internal magnetic-barrier of the rotor plays the role of field modulating and coupling between the internal stator's power and control windings. The non-magnetic ring plays the role of magnetic isolation and support. Therefore, the internal and external magnetic circuits in the electric machine are mutually independent. Meantime, the external unit electric machine (EUEM) is composed by the external stator, external air-gap and external magnetic-barrier. The internal unit electric machine (IUEM) is composed by the internal stator, internal air-gap and rotor internal magnetic-barrier. Equivalent salient number of poles in the rotor is the sum of the power and control windings pole pair number in [27–29], which is represented:

$$p_r = p_p + p_c \,, \tag{4}$$

where p_r expresses the equivalent salient number of poles in rotor.

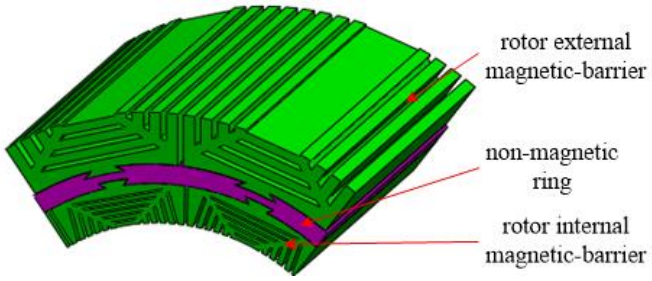

Fig. 3. Rotor configuration

2.3. Power flow

The proposed DSBDFG can be widely used in sub-synchronous, natural synchronous and super-synchronous of wind power. The output power of power windings in DSBDFG is directly flowed to the grid. However, the output power of the control windings could be flowed bidirectional. When the electric machine runs at super-synchronous speed, the output powers of power and control windings for the DSBDFG are fed back to the power grid, which is displayed in Fig. 4, where P_{empo} and P_{emco} stands for the external power and control windings absorbed mechanical power respectively, while P_{empi} and P_{emci} express the internal power and control windings absorbed mechanical power respectively, P_p and P_c express the power and control windings output power, P_{mec} express the input mechanical power, P_{mecp} and P_{mecc} express the power and control windings absorbed mechanical power, respectively. Under the super-synchronous operation of electric machine conditions, the power subsystem (P_{empo}, P_{empi}) absorbs the mechanical power (P_{mecp}) to convert into the electric power (P_p). The control subsystem (P_{emco}, P_{empi}) absorbs the mechanical power (P_{mecc}) to convert into the electric power (P_c).

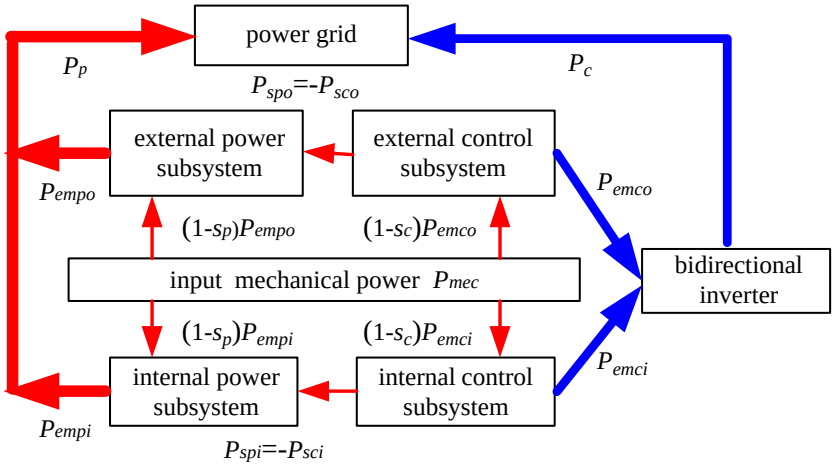

Fig. 4. Power flow of DSBDFG

The power flow direction in these three running modes of electric machine with ignoring copper loss can be summed up Table 1, where s_p and s_c represent power and control winding slip rate, respectively.

Table 1. Power flow direction of DSBDFG

Operating mode	Power flow	Running state
Sub-synchronous	P_{empo}, P_{empi}, P_{spo}, P_{spi}, $-P_{sco}$, $-P_{sci}$, P_{emcc}, P_p, $-P_c$	$0 < s_p < 1$, $s_c > 1$
Nature synchronous	P_{empo}, P_{empi}, P_{spo}, P_{spi}, $-P_{sco}$, $-P_{sci}$, P_{emcc}, P_p, $P_c = 0$	$0 < s_p < 1$, $s_c \to \infty$
Super-synchronous	P_{empo}, P_{empi}, P_{spo}, P_{spi}, P_{sco}, P_{sci}, P_{emcc}, P_p, P_c	$0 < s_p < 1$, $s_c < 1$

Note: The absorbed electric power is expressed by "–", otherwise, it is expressed output electric power.

3. Design and analysis of DSBDFG

This part focuses on the design-related problems, such as the power distribution, the principal dimension, the rotor coupling capability and the steady-state analysis. The design flowchart of the DSBDFG with the magnetic-barrier rotor is given in Fig. 5.

Based on the electric machine design flowchart, combined with the design method and requirements, a 50 kW DSBDFG is designed, whose principal dimension is given in Table 2.

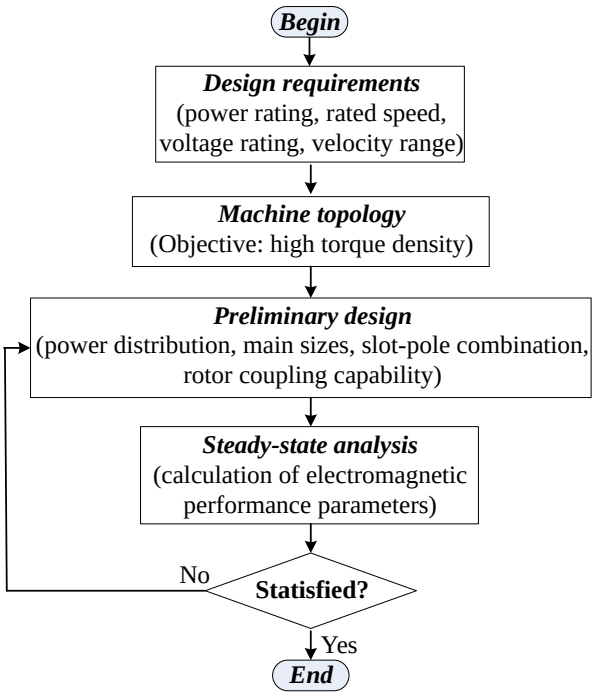

Fig. 5. Design flowchart of DSBDFG

Table 2. Principal dimensions of electric machine

Parameters	Value
Voltage rating (V)	400
Power and control windings pole-pairs number	6, 4
Speed range (r/min)	210~390
External stator external and internal diameter (mm)	800, 630
Internal stator external and internal diameter (mm)	400, 220
Iron core axial length (mm)	330
Rotor external and internal diameter (mm)	628.1, 401.2
External and internal stator slots number	144, 72

3.1. Sub-synchronous running

The power source phase sequence of the power windings is contrary to that of the control windings in sub-synchronous running. The control windings assimilate electrical supply and mechanical energy, which is consumed with the rotor circuit and itself. According to the principal dimensions of design electric machine, the performance parameters of the DSBDFG are analyzed

and calculated to adopt the FEM at 240 rpm and load, and the results are illustrated in Figs. 6 and 7. From the result, the EMFs of external and internal power windings in electric machine with load are 1.97% and 0.76% larger than voltage rating, respectively. Meanwhile, the EMF phase angles of the external and internal power windings are basically consistent. Therefore, the results meet the winding connecting requirements of the design electric machine. Figure 6(b) depicts A-phase load voltage and current. Figure 7 illustrates the relationship of output power and load current.

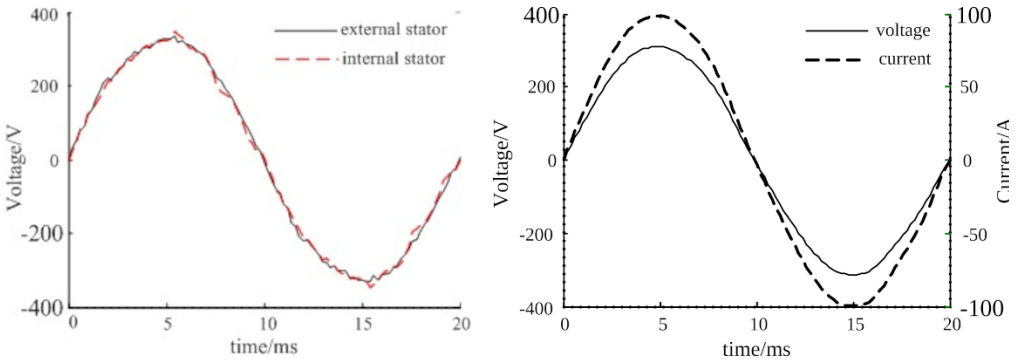

Fig. 6. Voltage and current in DSBDFG with load (240 rpm): PW phase EMF (240 rpm) (a); load voltage and current (240 rpm) (b)

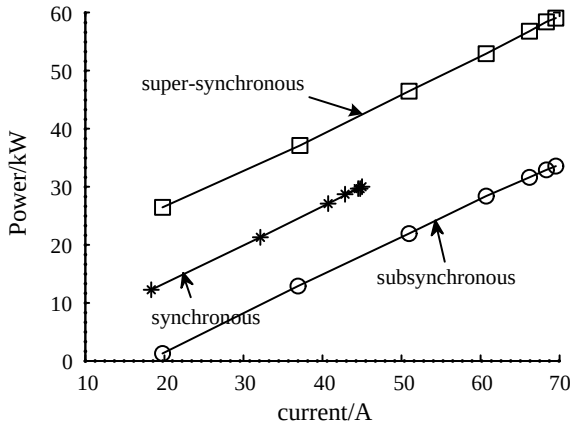

Fig. 7. Relationship of output power and current

3.2. Synchronous running

When the power grid energy is fed by the power windings, the control windings are supplied by the direct-current power supply. The power frequency of the control windings is equal to zero.

Therefore, the rotor speed of electric machine is illustrated in Formula (5):

$$n_r = \frac{60 f_p}{p_p + p_c}. \tag{5}$$

When operating in synchronous status, the DSBDFG with load is studied on operating at the speed of 300 rpm, and the result is displayed in Fig. 8. From the result, the EMF phase angle of external power winding is basically the same as that of internal power winding.

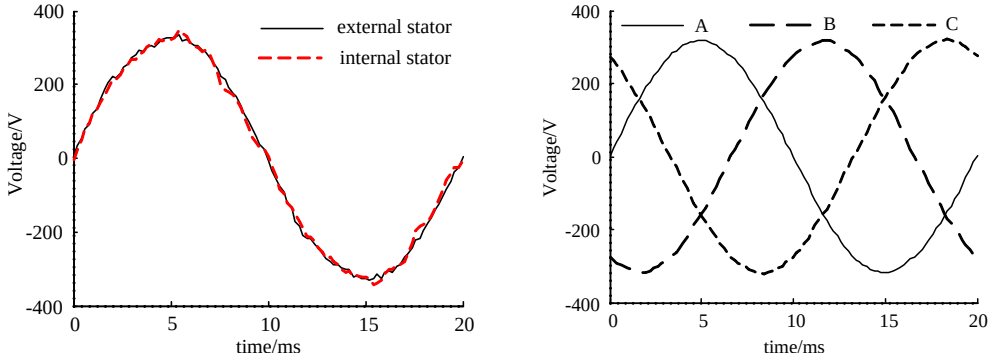

Fig. 8. Winding EMF and load voltage: PW phase EMF (a); load phase voltage (b)

However, the power winding voltage of external stator is 1.19% higher than that of internal stator. The current curve is not given in this paper because load is resistance. Through the results analysis and comparison, the results verify winding connecting mode and Eq. (3). The relationship of output power and load current is shown in Fig. 7.

3.3. Super-synchronous running

3.3.1. No load

The control and power windings current sequences are the same as electric machine with the super-synchronous running. The DSBDFG with no load is adopted to the FEM at the 360 rpm to calculate and discuss air-gap magnetic flux density, power windings phase electromagnetic force (EMF) and magnetizing characteristics, and the result is illustrated in Figs. 9–11. From the result, the relative error of external and internal air-gaps magnetic flux densities is less than 0.55%. The EMF of external power windings is 1.31% larger than the voltage rating. However, the EMF of internal power windings is 0.52% lower than the voltage rating. Meanwhile, the EMF phase angles of the external and internal power windings are the basically consistent. Through the analysis of results, it meets the requirements of the electromagnetic characteristics consistency in the design electric machine.

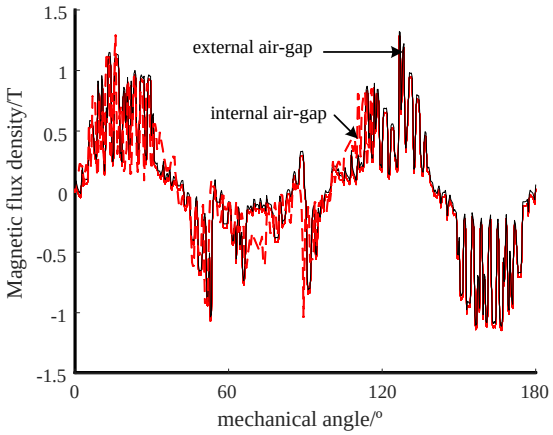

Fig. 9. Air-gap magnetic flux density of DSBDFG

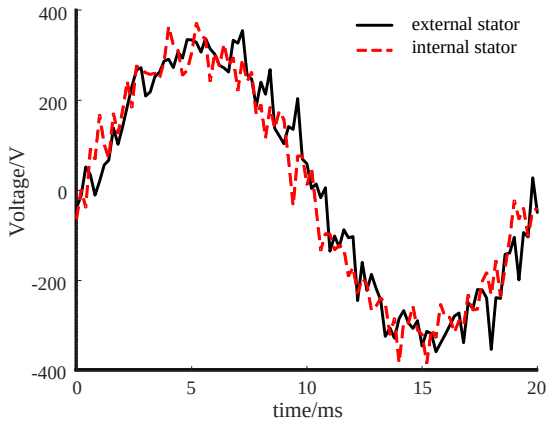

Fig. 10. PW phase EMF of DSBDFG with no load

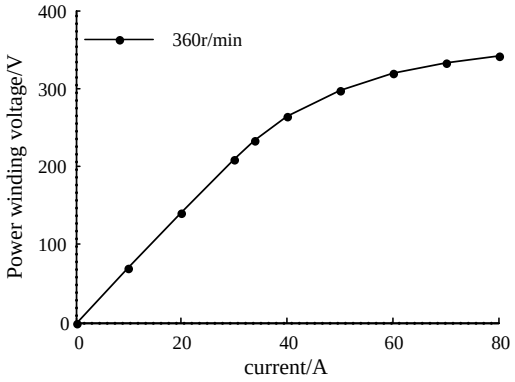

Fig. 11. Magnetizing characteristics of DSBDFG

3.3.2. Load operation

The DSBDFG with load is studied on the magnetic field distribution, air-gap magnetic flux density, winding phase EMF, load voltage and current at 360 rpm, and the results are illustrated in Figs. 12–15.

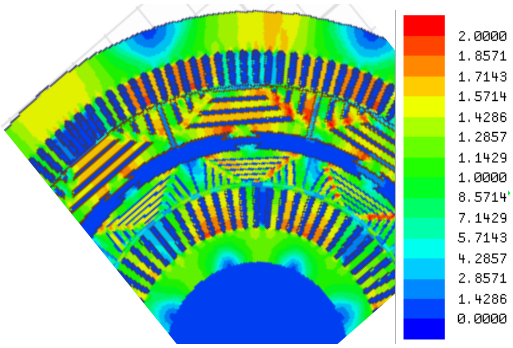

Fig. 12. Magnetic field distribution of electric machine

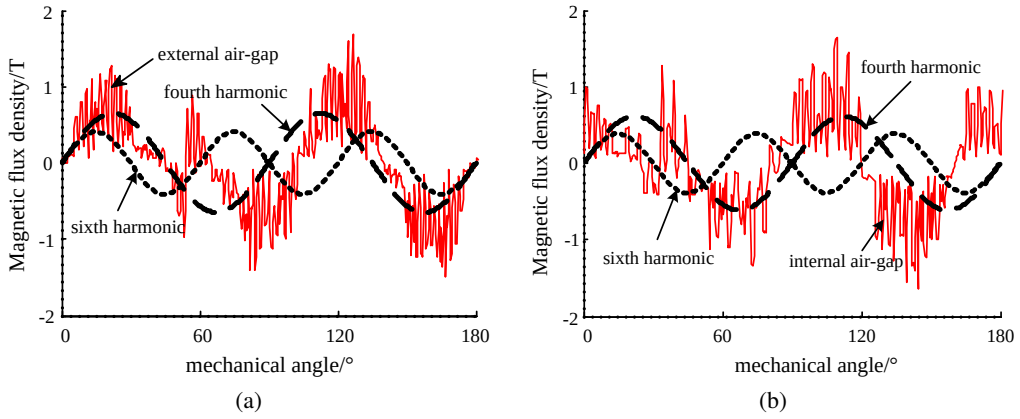

Fig. 13. DSBDFG air-gap flux density: external air-gap magnetic flux density (a); internal air-gap magnetic flux density (b)

From the result, the magnetic field distribution meets the design requirements of electric machine. Meanwhile, the fourth and sixth harmonics are the control and power windings fundamental harmonic, respectively. At the same time, it is the useful harmonics of air-gap magnetic flux density. The magnetic flux densities of the external and internal air-gaps are 0.6232 T and 0.6152 T, respectively. The internal air-gap magnetic flux density of the DSBDFG is 1.28% lower than the external air-gap magnetic flux density, which meets the design requirements of the electric machine.

Figure 14 is the external and internal power winding phase EMFs of electric machine with load. Through the analysis of results, the external and internal power winding EMFs are 3.62%

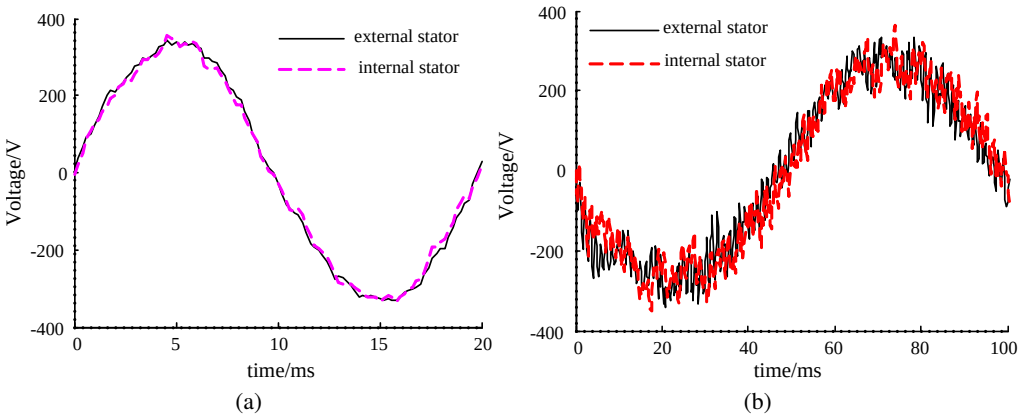

Fig. 14. Winding phase EMF of DSBDFG with 360 rpm: PW phase EMF (a); CW phase EMF (b)

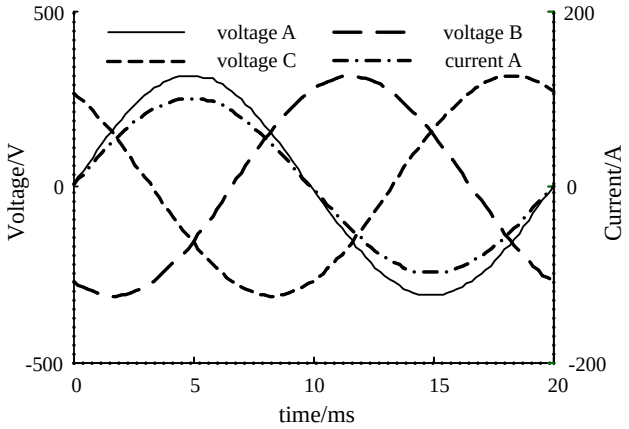

Fig. 15. Load phase voltage and current of DSBDFG with 360 rpm

and 0.94% larger than the voltage rating, respectively. However, the EMF of external control winding is 0.59% lower than that of internal control windings. However, the EMF phase angles of external and internal power windings are basically consistent. Meantime, the EMF phase angles of external and internal control windings are also basically. The relation of output power and current is illustrated in Fig. 7. Figure 15 is the load voltage and current. From the result, the phase voltage and current are 220 V and 71 A, respectively. Meanwhile, the relative error of three-phase winding voltage is less than 1%. By analyzing the results, the proposed DSBDFG met the requirements of design and winding connecting.

Under the same load and exciting current conditions, the DSBDFG is studied on the relationship of output power and speed, and the result is shown in Fig. 16. From the result, under the same load and exciting current conditions, the output power of the DSBDFG increases with the increase of speed.

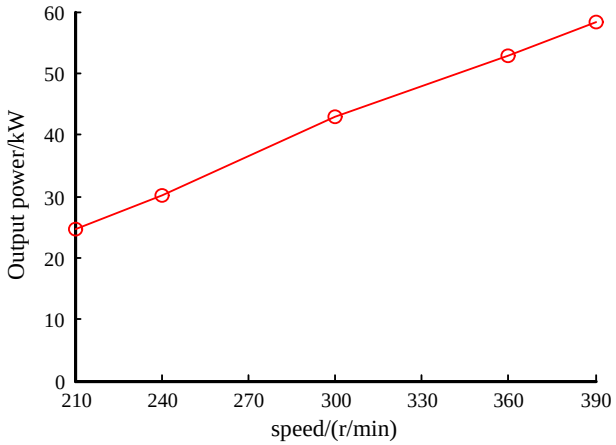

Fig. 16. Relationship of output power and speed in the DSBDFG

4. Conclusion

The paper particularly illustrates the different running modes of the DSBDFG application for wind power generation. Based on the topological structure and working principle of electric machine, the winding connecting, the rotor topology and the power flow of the DSBDFG are discussed and analyzed. After that, a 50 kW DSBDFG is designed. According to the electric machine principal dimensions, the parameters of electric machine are calculated to adopt the numerical method in the different running modes, such as air-gap magnetic flux density, winding phase EMF, field distribution and load voltage and current. The results meet the electromagnetic characteristics consistency and winding connecting requirements of the design electric machine. Likewise, it verifies the proposed DSBDFG has a strong ability of speed governing.

Acknowledgements

The authors want to say thanks to the funding support from the Key Scientific Research Projects of Higher Education Institutions of Henan Province (22A470004), Natural Science Foundation of Henan Province (222300420400), Science and Technology Research Project of Henan Province (232102320053), Research and Practice of Higher Education Teaching Reform (2021JGPY031) and Research Teaching Demonstration Course (YJXKC202204).

References

[1] https://www.163.com/dy/article/G60BD0A90514C30V.html, accessed March 2021.

[2] Holtslag M.C., Bierbooms W.A.A.M., van Bussel G.J.W., *Extending the diabatic surface layer wind shear profile for offshore wind energy*, Renewable Energy, vol. 101, pp. 96–110 (2017), DOI: 10.1016/j.renene.2016.08.031.

[3] Selin Karlilar, Firat Emir, *Exploring the role of coal consumption, solar, and wind power generation on ecological footprint: evidence from India using Fourier ADL cointegration test*, Environmental Science and Pollution Research, vol. 30, no. 9, pp. 24077–24087 (2022), DOI: 10.1007/s11356-022-23910-z.

[4] http://www.chinacrane.net/news/202011/07/181900.html, accessed November 2020.

[5] https://news.bjx.com.cn/html/20230417/1301287.shtml, accessed April 2023.

[6] Ge Xiaolin, Chen Quan, Fu Yang *et al.*, *Stochastic maintenance path planning for offshore wind turbines considering wake effects*, Acta Energiae Solaris Sinica, vol. 42, no. 12, pp. 183–191 (2021), DOI: 10.1093/icb/40.6.925.

[7] Olubamiwa Oreoluwa I., Gule Nkosinathi, *A review of the advancements in the design of brushless doubly fed machines*, Energies, vol. 15, no. 3, 725 (2022), DOI: 10.3390/en15030725.

[8] Ronghai Qu, Yingzhen Liu, Jin Wang, *Review of superconducting generator topologies for direct-drive wind turbines*, IEEE Transactions on Applied Superconductivity, vol. 23, no. 3, 5201108 (2013), DOI: 10.1109/TASC.2013.2241387.

[9] Yasser Belkacem, Said Drid, Abdesslam Makouf, Larbi Chrifi-Alaoui, *Multi-agent energy management and fault tolerant control of the micro-grid powered with doubly fed induction generator wind farm*, International Journal of System Assurance Engineering and Management, vol. 13, no. 1, pp. 267–277 (2022), DOI: 10.1007/s13198-021-01228-2.

[10] Miaohong Su, Haiying Dong, Kaiqi Liu, Weiwei Zou, *Subsynchronous oscillation and its mitigation of VSC-MTDC with doubly-fed induction generator-based wind farm integration*, Archives of Electrical Engineering, vol. 70, no. 1, pp. 53–72 (2021), DOI: 10.24425/aee.2021.136052.

[11] Hamidreza Mosaddegh Hesar, Hossein Abootorabi Zarchi, Gholamreza Arab Markadeh, *Modeling and dynamic performance analysis of brushless doubly fed induction machine considering iron loss*, IEEE Transactions on Energy Conversion, vol. 35, no. 1, pp. 193–202 (2020), DOI: 10.1109/TEC.2019.2944424.

[12] Hao Liu, *Electromagnetic design and characteristic analysis of dual-stator brushless doubly-fed wind power generator with cage-barrier rotor*, PhD Thesis, School of Electrical Engineering, Shenyang University of Technology, Shenyang (2020).

[13] Sajjad Tohidi, *Analysis and simplified modeling of brushless doubly-fed induction machine in synchronous mode of operation*, IET Electric Power Applications, vol. 10, no. 2, pp. 110–116 (2016), DOI: 10.1049/iet-epa.2015.0217.

[14] Roland Ryndzionek, Krzysztof Blecharz, Filip Kutt, MichałMichna, Grzegorz Kostro, *Development and performance analysis of a novel multiphase doubly-fed induction generator*, Archives of Electrical Engineering, vol. 71, no. 4, pp. 1003–1015 (2022), DOI: 10.24425/aee.2022. 142121.

[15] Resmi R., Vanitha V., Nambiar T.N.P., Sasi K. Kottayil, *Design and implementation of brushless doubly fed induction machine with new stator winding configuration*, Wind Engineering, vol. 45, no. 1, pp. 11–23 (2021), DOI: 10.1177/0309524X19868423.

[16] Hao Liu, Yue Zhang, Shi Jin, Fengge Zhang, Heng Nian, He Zhang, *Electromagnetic design and optimization of dual-stator brushless doubly-fed wind power generator with cage-barrier rotor*, Wind Energy, vol. 22, no. 6, pp. 713–731 (2019), DOI: 10.1002/we.2317.

[17] Ademi Sul, Jovanovic Milutin, *High-efficiency control of brushless doubly-fed machines for wind turbines and pump drives*, Energy Conversion and Management, vol. 81, no. 1, pp. 120–132 (2014), DOI: 10.1016/j.enconman.2014.01.015.

[18] Liu Guangjun, Wang Xuefan, *Design and performance analysis of a 700-kW wound-rotor BDFIG for ship shaft generator application*, IEEJ Transactions on Electrical and Electronic Engineering, vol. 11, no. 1, pp. 112–123 (2016), DOI: 10.1002/tee.22195.

[19] Ruviaro Mauricio, Runcos Fredemar, *Analysis and test results of a brushless doubly fed induction machine with rotary transformer*, IEEE Transactions on Industrial Electronics, vol. 59, no. 6, pp. 2670–2677 (2012), DOI: 10.1109/TIE.2011.2165457.

[20] Han Peng, Cheng Ming, Chen Zhe, *Dual-electrical-port control of cascaded doubly-fed induction machine for EV/HEV applications*, IEEE Transactions on Industry Applications, vol. 53, no. 2, pp. 1390–1398 (2017), DOI: 10.1109/TIA.2016.2625770.

[21] Peng Han, Ming Cheng, Rensong Luo, *Design and analysis of a brushless doubly-fed induction machine with dual-stator structure*, IEEE Transactions on Industrial Electronics, vol. 31, no. 3, pp. 1132–1141 (2016), DOI: 10.1109/TEC.2016.2547955.

[22] Chukwuemeka Chijioke Awah, *Performance comparison of double stator permanent magnet machines*, Archives of Electrical Engineering, vol. 71, no. 4, pp. 829–850 (2022), DOI: 10.24425/aee.2022.142111.

[23] Zhang Changguo, Cheng Ming, Zeng Yu, *Design and analysis of dual-stator brushless doubly-fed generator for wind turbine*, IEEJ Transactions on Electrical & Electronic Engineering, vol. 17, no. 2, pp. 276–286 (2022), DOI: 10.1002/tee.23503.

[24] Hao Wang, Siyang Yu, Shi Jin, Fengge Zhang, *Electromagnetic and mechanical design of module dual stator brushless doubly-fed generator for offshore wind turbine*, IET Renewable Power Generation, vol. 15, no. 3, pp. 631–640 (2021), DOI: 10.1049/rpg2.12050.

[25] Hao Liu, Fengge Zhang, Rui Dai, *Air-gap magnetic field analysis of dual-stator brushless doubly-fed generator based on analytic method*, 2019 IEEE Transportation Electrification Conference and Expo, Asia-Pacific, ITEC Asia-Pacific 2019, Seogwipo, Korea, pp. 1–6 (2019).

[26] Xiaodong Jiang, Fengge Zhang, Rui Dai, *Thermal analysis and calculation of double stator brushless doubly-fed generator for wind power generation*, 2019 IEEE Transportation Electrification Conference and Expo, Asia-Pacific, ITEC Asia-Pacific 2019, Seogwipo, Korea, pp. 1–5 (2019).

[27] Hamed Gorginpour, Hashem Oraee, Ehsan Abdi *et al.*, *Calculation of core and stray load losses in brushless doubly fed induction generators*, IEEE Transactions on Industrial Electronics, vol. 61, no. 7, pp. 3167–3177 (2014), DOI: 10.1109/TIE.2013.2279357.

[28] Fengxiang Wang, Fengge Zhang, *Brushless doubly-fed AC electric machine with magnetic field modulated*, Jilin University Press (2004).

[29] Yiding Wang, Jianhui Su, Jidong Lai *et al.*, *Equivalent and identification of integrated coupling parameter of variable speed constant frequency brushless doubly fed generator*, Journal of Power Electronics, vol. 22, no. 1, pp. 61–71 (2022), DOI: 10.1007/s43236-021-00346-1.